

NASA EOS Aqua Satellite AMSR-E Data for Snow Variation

Boori MS^{1*}, Ferraro RR² and Voženílek V³

¹National Research Council (NRC), USA

²NOAA/NESDIS/STAR/ Satellite Climate Studies Branch and Cooperative Institute for Climate and Satellites (CICS), ESSIC, University of Maryland, College Park, Maryland, USA

³Palacky University Olomouc, 17.listopadu 50, 771 46 Olomouc, Czech Republic

NASA EOS Aqua satellite AMSR-E data were used for snow variation study in Northern Hemisphere (NH) from 2007 to 2011 for January, April, July and October months with 500 m elevation difference. Monitoring of the seasonal snow cover with different elevation is important for several purposes such as climatology, hydrometeorology, water use and control and hydrology, including flood forecasting and food production.

The objective of this study was to analyze the seasonal snow type and snow cover changes on the NH and its relations with different elevation. Such information is urgently need for the satellite precipitation community to better delineate snow covered regions to minimize the impact of falsely classifying raining areas from snow on the ground [1,2]. This type of research work is also useful to improve the quality of future NASA satellite data [3]. This paper describes an approach to assemble a consistent 5-year record of seasonal snow covered area of NH. There are, however, very limited data that can be used to corroborate our findings (satellite data, secondary data or otherwise), making extensive quantitative validation of the snow estimates extremely challenging [4].

The methodology involves conversion of NASA EOS Aqua satellite AMSR-E SWE data into 6 snow classes, computation of NDSI, determination of the boundary between snow classes from spectral response data and threshold slicing of the image data [5]. Accuracy assessment of AMSR-E snow products was accomplished using Geographic Information System (GIS) techniques. There are many techniques available for detecting and recording differences, such as image differencing, ratios and correlation [6,7]. However, the simple detection of change is rarely sufficient in itself: information is generally required about the initial and final snow cover analysis as described by [8].

Furthermore, detection of image differences may be confused with problems in penology and cropping and such problems may be exacerbated by limited image availability, poor quality in temperate zones and difficulties in calibrating poor images [9]. Post-classification comparisons of derived, thematic maps go beyond simple change detection because they attempt to quantify the different types of change [10]. Their degree of success depends upon the reliability of the maps that have been made by image classification. Broadly speaking, both large scale changes such as very low snow class, and small scale changes like extreme snow, might be mapped reasonably easily [11,12].

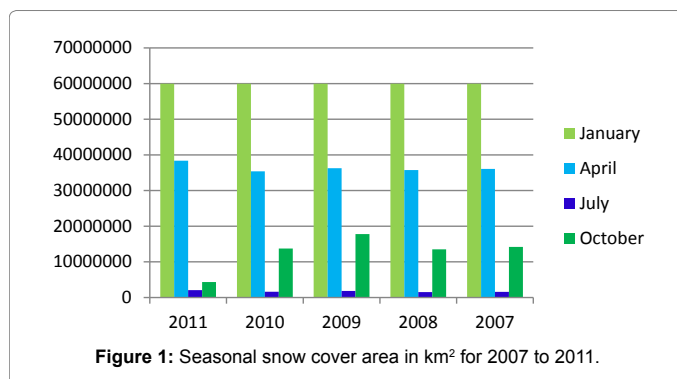


Figure 1: Seasonal snow cover area in km² for 2007 to 2011.

Data and Image Classification

The Advanced Microwave Scanning Radiometer - Earth Observing System (AMSR-E) is a twelve-channel, six-frequency, passive-microwave radiometer system. It measures horizontally and vertically polarized brightness temperatures at 6.9, 10.7, 18.7, 23.8, 36.5 and 89.0 GHz. Spatial resolutions of the individual measurements varies from 5.4 km at 89 GHz to 56 km at 6.9 GHz. AMSR-E improves upon past microwave radiometers. The monthly level-3 AMSR-E snow water equivalent (SWE) data AE MoSno (AMSR-E/Aqua monthly L3 Global Snow Water Equivalent EASE-Grids) in Northern Hemisphere were obtained from the NSIDC NASA website [13-15]. These data are stored in Hierarchical Data Format-Earth Observing System (HDF-EOS) format and contain SWE data and quality assurance flags mapped to 25 km Equal-Area Scalable Earth Grids (EASE-Grids). Actual SWE values are scaled down by a factor of 2 for storing in the HDF-EOS file, resulting in a stored data range of 0-240. Users must multiply the SWE values in the file by a factor of 2 to scale the snow depth data up to the correct range of 0-480 mm. Finally Shuttle Radar Topography Mission (SRTM) data of approximately 90 m resolution were downloaded from the website and used to prepare the digital elevation map (DEM) [16].

Unsupervised classification was performed here using 0 to 255 gray levels and digital topographic maps. All AMSR-E monthly SWE images were transformed into ESRI grid format files with Lambert Azimuthal equal area projection and the grid was re-sampled by binary approach [17,18]. The end gray levels from 240 to 255 of AMSR-E data indicates a snow free surface (or land surface), off-earth, land or snow impossible, ice sheet, water and data missing, respectively. In terms of snow depth each gray level need to multiply by factor 2 so this data show snow depth from 0 to 480 mm [19,20].

Spatial-temporal Variability of Snow Covers with Elevation

Snow cover classification was computed from 2007 to 2011 for the months of January, April, July and October (Figure 1). Separate analyses were done for 500 m elevation ranges. The snow was classified into six main classes based on SWE values: Very low snow, low snow, medium snow, high snow, very high snow and extreme snow and land which was covered by snow in winter but not in other seasons was classified as "No Snow" class (Figure 2).

*Corresponding author: Mukesh Singh Boori, Palacky University Olomouc, 17 listopadu 50, 771 46 Olomouc, Czech Republic, Tel: 420585631111; E-mail: mukesh.boori@upol.cz

Received June 25, 2014; Accepted June 26, 2014; Published June 30, 2014

Citation: Boori MS, Ferraro RR, Voženílek V (2014) NASA EOS Aqua Satellite AMSR-E Data for Snow Variation. J Geol Geosci 3: e116. doi: 10.4172/2329-6755.1000e116

Copyright: © 2014 Boori MS, et al. This is an open-access article distributed under the terms of the Creative Commons Attribution License, which permits unrestricted use, distribution, and reproduction in any medium, provided the original author and source are credited.

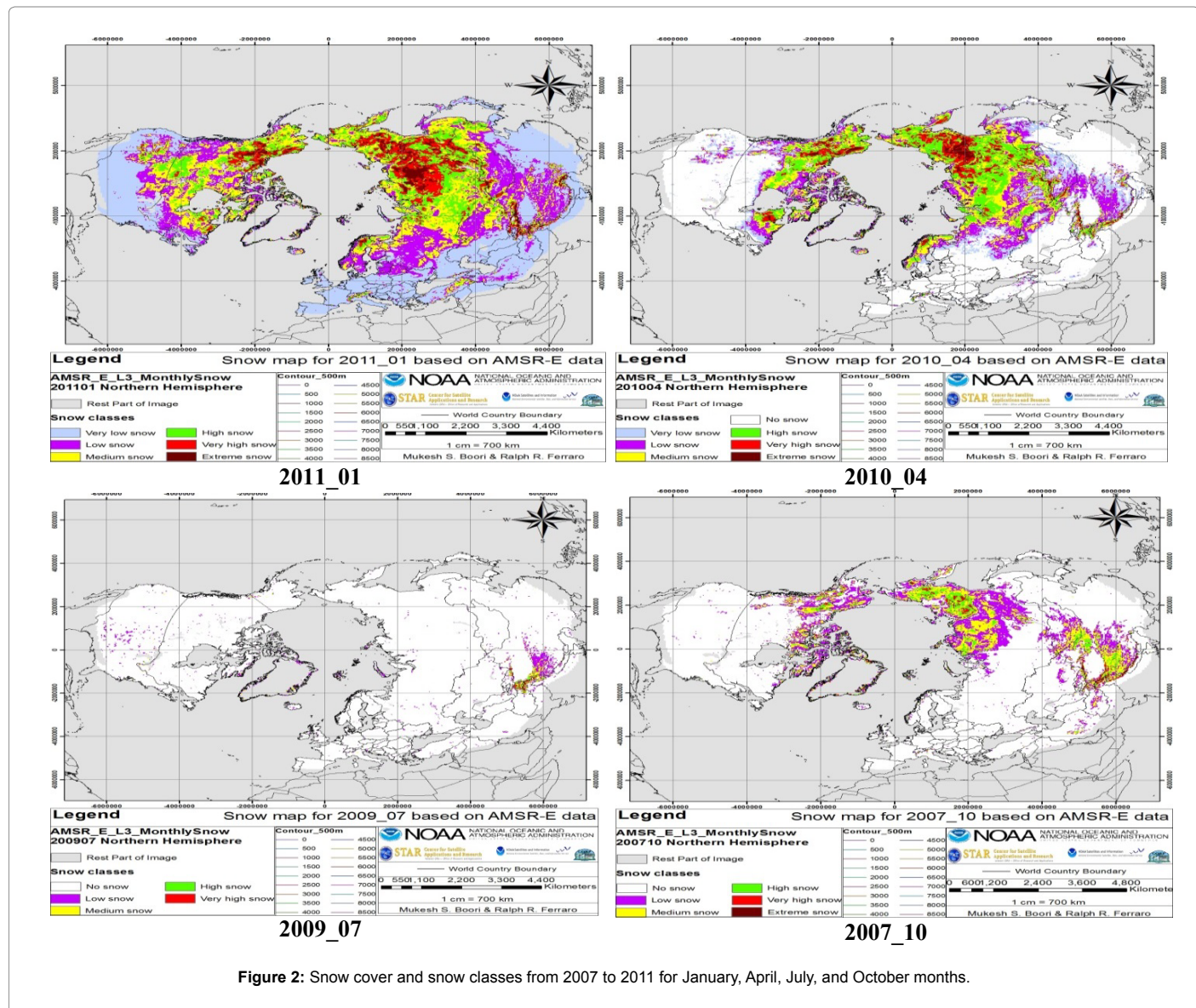


Figure 2: Snow cover and snow classes from 2007 to 2011 for January, April, July, and October months.

	2011_01			2010_01			2009_01			2008_01			2007_01		
Class	Area	%													
Very low snow	21.9	36.4		21.4	35.7		22.2	37.0		21.7	36.2		24.3	40.6	
Low snow	13.4	22.3		13.2	21.9		15.1	25.1		14.8	24.7		13.2	22.1	
Medium snow	11.5	19.1		11.2	18.7		11.2	18.7		11.9	19.9		11.4	19.0	
High snow	7.5	12.5		8.6	14.4		6.7	11.1		6.7	11.2		6.3	10.5	
Very high snow	4.3	7.2		4.4	7.3		3.7	6.1		3.5	5.8		3.6	5.9	
Extreme snow	1.5	2.5		1.2	2.0		1.2	1.9		1.3	2.2		1.2	1.9	
Total snow	60.0	100.0													
RPI	264.9			264.9			264.9			264.9			264.9		
Total	324.8														
2011_04				2010_04			2009_04			2008_04			2007_04		
Class	Area	%	%												
Very low snow	10.7	27.8	17.8	8.6	24.2	14.3	8.8	24.3	14.7	9.5	26.6	15.9	9.6	26.7	16.0
Low snow	9.8	25.6	16.4	8.9	25.1	14.8	8.9	24.5	14.8	8.8	24.6	14.6	9.3	25.8	15.5
Medium snow	7.7	20.0	12.8	8.3	23.5	13.9	8.2	22.6	13.7	7.4	20.6	12.3	7.5	20.9	12.6
High snow	5.5	14.4	9.2	6.0	16.8	9.9	5.9	16.3	9.9	5.9	16.5	9.8	5.3	14.6	8.8

Table 1: Snow classes and snow cover area in million km² for January, April, July and October months from 2007 to 2011.

The coldest month has all six snow type classes due to snow pack growth whereas the summer months only contain residual snow at the highest elevations. Sharp season-to-season differences were noted. The final results show the greatest snow cover extent in January whereas total snow in April is 60%, July 3% and in October near to 25% (Table 1). In terms of inter-seasonal variations during the study period, the minimum (1.53 million km²) snow cover extent was observed in July 2008 and the maximum (60.0 km²) in January 2010 (Figure 2). In terms of elevation, in January snow covered area represent more than 70% of surfaces with altitudes in between 0 to 2000m, and in summer more than 70% for altitudes higher than 5000m and it's totally constant at altitude from 7000m and above (Figure 3 and Table 2).

The seasonal snow cover extent changes from 2007 to 2011 were successfully monitored by NASA EOS Aqua satellite AMSR-E data. Finally, this study shows how NASA EOS Aqua satellite AMSR-E data can be useful for the long-term observation of the intra and inter-annual variability of snow packs in rather inaccessible regions and providing useful information on a critical component of the hydrological cycle, where the network of meteorological stations is deficient.

References

1. Boori MS, Vozenilek V (2014) Land use/cover, vulnerability index and exposure intensity. *Journal of Environments* 1: 1-7.
 2. Boori MS, Vozenilek V (2014) Remote sensing and GIS for Socio-hydrological vulnerability. *Journal of Geology and Geosciences* 3: 1-4.
 3. Singh A (1989) Digital change detection techniques using remotely sensed data. *International Journal of Remote Sensing* 10: 989-1003.

4. Boori MS, Vozenilek V, Burian J (2014) Land-cover disturbances due to tourism. Proceedings of the Fifth International Conference on Innovations in Bio-Inspired Computing and Applications IBCA 2014. Springer International Publishing 63-72.
 5. Brus J, Boori MS, Vozenilek V (2013) Detection and visualizations of ecotones important landscape pattern under uncertainty. *Journal of Earth Science and Climate Change* 4: 1-4.
 6. Boori MS, Ferraro RR (2013) Microwave polarization and gradient ratio (MPGR) for global land surface phenology. *Journal of Geology and Geosciences* 2: 1-10.
 7. Boori MS, Ferraro RR (2012) Northern Hemisphere snow variation with season and elevation using GIS and AMSR-E data. *Journal of Earth Science and Climate Change* S12: 1-6.
 8. Boori MS, Amaro VE, Targino A (2012) Coastal risk assessment and adaptation of the impact of sea-level rise, climate change and hazards: A RS and GIS based approach in Apodi-Mossoro estuary, Northeast Brazil. *International Journal of Geomatics and Geosciences* 2: 815-832.
 9. Ferraro R (1997) SSM/I derived global rainfall estimates for climatological applications. *J Geophys Res* 102, 16 715-735.
 10. Boori MS (2011) Avaliação do impacto ambiental e gestão dos recursos naturais no estuário Apodi/Mossoró, nordeste do Brasil. Library thesis from Federal University of Rio Grande do Norte, Brazil.
 11. Boori MS, Amaro VE (2011) Natural and eco-environmental vulnerability assessment through multi-temporal satellite data sets in Apodi valley region, Northeast Brazil. *Journal of Geography and Regional Planning* 4: 216- 230.
 12. Boori MS, Amaro VE (2011) A remote sensing and GIS based approach for climate change and adaptation due to sea-level rise and hazards in Apodi-Mossoro estuary, Northeast Brazil. *International Journal of Plant, Animal and Environmental Sciences* 1: 14-25.

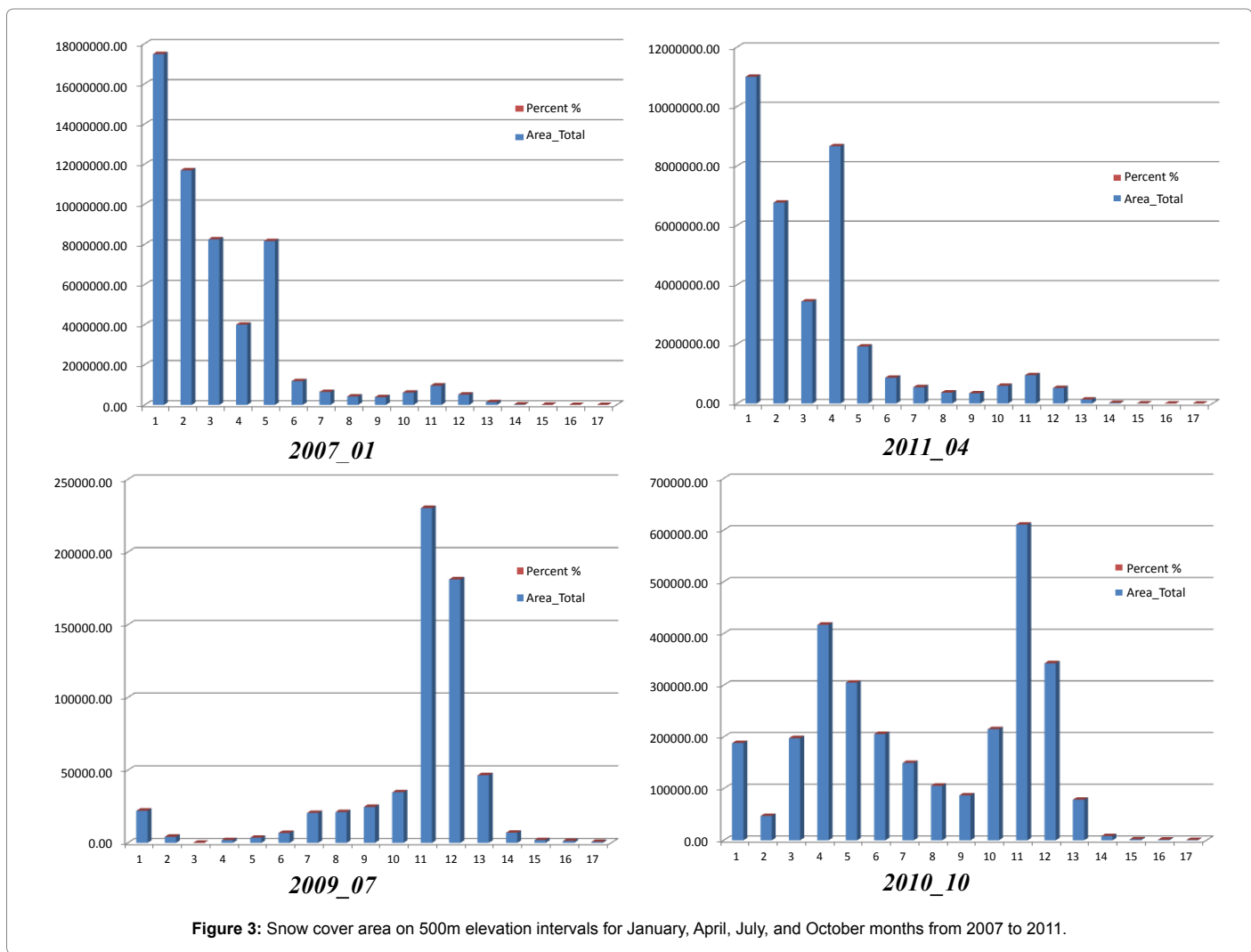


Figure 3: Snow cover area on 500m elevation intervals for January, April, July, and October months from 2007 to 2011.

Contour	2011_07		2010_07		2009_07		2008_07		2007_07	
	Area	%	Area	%	Area	%	Area	%	Area	%
0	24977.1	5.1	16251.0	3.2	22070.7	3.6	17640.8	3.7	19238.2	3.7
500	9376.2	1.9	5903.8	1.2	4172.7	0.7	4828.9	1.0	6057.8	1.2
1000	3766.8	0.8	0.0	0.0	0.0	0.0	1486.4	0.3	0.0	0.0
1500	2717.8	0.6	1885.1	0.4	1885.1	0.3	3164.3	0.7	2513.5	0.5
2000	4927.9	1.0	3494.8	0.7	3494.8	0.6	2640.4	0.5	2238.0	0.4
2500	3374.0	0.7	3374.0	0.7	6714.0	1.1	1256.8	0.3	628.4	0.1
3000	17821.4	3.7	4172.7	0.8	20510.6	3.4	6686.2	1.4	6686.2	1.3
3500	21783.6	4.5	10230.5	2.0	21139.0	3.5	16740.3	3.5	16111.9	3.1
4000	25537.6	5.2	10230.5	2.0	24683.3	4.1	16111.9	3.4	14855.2	2.8
4500	36174.2	7.4	29109.8	5.8	34737.4	5.7	26568.4	5.5	29533.9	5.7
5000	159247.9	32.7	207542.1	41.2	230191.7	37.9	191164.9	39.8	223048.0	42.7
5500	119869.5	24.6	149102.7	29.6	181150.1	29.8	140140.4	29.2	152697.2	29.3
6000	49246.4	10.1	53054.7	10.5	46500.2	7.6	42377.8	8.8	40100.9	7.7
6500	6686.2	1.4	6283.8	1.2	6912.2	1.1	7314.6	1.5	6283.8	1.2
7000	628.4	0.1	628.4	0.1	1885.1	0.3	1256.8	0.3	628.4	0.1
7500	628.4	0.1	1285.1	0.3	1256.8	0.2	628.4	0.1	628.4	0.1
8000	628.4	0.1	628.4	0.1	628.4	0.1	628.4	0.1	628.4	0.1
Total	487391.7	100.0	503177.3	100.0	607931.9	100.0	480635.6	100.0	521878.2	100.0
2011_09		2010_10		2009_10		2008_10		2007_10		
Contour	Area	%	Area	%	Area	%	Area	%	Area	%
0	111976.6	6.8	188062.3	6.4	533296.6	10.9	185548.8	5.9	218392.8	6.7

500	41247.1	2.5	47128.6	1.6	952328.4	19.4	47531.0	1.5	109753.1	3.4
1000	126556.5	7.7	197488.0	6.7	390727.4	8.0	197714.0	6.3	236673.6	7.3
1500	184694.4	11.2	417068.5	14.1	573907.7	11.7	388305.3	12.3	454947.7	14.0
2000	145332.4	8.8	304891.6	10.3	359504.6	7.3	302405.9	9.6	321080.9	9.9
2500	112882.6	6.8	205480.5	6.9	218952.8	4.5	223351.5	7.1	249665.3	7.7
3000	100544.6	6.1	149656.5	5.1	185774.7	3.8	169803.2	5.4	176804.6	5.4
3500	50474.8	3.1	105568.0	3.6	121933.7	2.5	115423.9	3.7	117507.2	3.6
4000	50877.1	3.1	86920.8	2.9	120108.8	2.5	103484.7	3.3	117683.6	3.6
4500	87929.9	5.3	214935.6	7.3	300326.2	6.1	275859.2	8.8	225362.6	6.9
5000	352463.8	21.3	610560.2	20.6	694321.3	14.2	678827.7	21.5	592111.2	18.2
5500	214404.7	13.0	342467.6	11.6	362801.7	7.4	364863.3	11.6	341210.8	10.5
6000	59696.2	3.6	78547.6	2.7	73520.6	1.5	87570.9	2.8	80432.7	2.5
6500	8169.0	0.5	8169.0	0.3	9425.7	0.2	8169.0	0.3	8797.3	0.3
7000	1885.1	0.1	1885.1	0.1	1885.1	0.0	1885.1	0.1	1885.1	0.1
7500	1256.8	0.1	1256.8	0.0	1256.8	0.0	1256.8	0.0	1256.8	0.0
8000	628.4	0.0	628.4	0.0	628.4	0.0	628.4	0.0	628.4	0.0
Total	1651019.9	100.0	2960714.9	100.0	4900700.4	100.0	3152628.5	100.0	3254193.8	100.0
			2011_01		2010_01		2009_01		2008_01	
Contour	Area	%								
0	17362649.6	32.6	17959009.5	33.0	16539754.7	30.7	17177288.2	32.7	17481910.7	32.1
500	9197864.9	17.3	10935393.3	20.1	10494707.4	19.5	9463614.5	18.0	11692291.3	21.5
1000	10294087.4	19.3	8425619.9	15.5	10313948.1	19.1	10085143.7	19.2	8252253.1	15.1
1500	4284155.9	8.0	4197795.3	7.7	4046441.8	7.5	6478086.7	12.3	4001756.6	7.3
2000	4800833.2	9.0	8012046.2	14.7	7669374.4	14.2	4443398.8	8.5	8167279.0	15.0
2500	3665846.9	6.9	1174627.0	2.2	1126771.6	2.1	1123920.2	2.1	1188233.3	2.2
3000	637913.4	1.2	628591.2	1.2	627988.2	1.2	645518.8	1.2	641266.3	1.2
3500	426450.2	0.8	400986.6	0.7	411614.3	0.8	430249.4	0.8	422342.9	0.8
4000	400835.7	0.8	405413.7	0.7	406438.4	0.8	393439.4	0.7	389942.0	0.7
4500	604524.6	1.1	580856.0	1.1	595727.4	1.1	581812.2	1.1	609286.1	1.1
5000	955138.9	1.8	951997.0	1.8	937544.2	1.7	971476.8	1.9	962679.4	1.8
5500	516529.0	1.0	524896.1	1.0	542921.1	1.0	525954.8	1.0	513200.8	0.9
6000	136987.0	0.3	138872.2	0.3	128189.7	0.2	131331.6	0.3	134473.5	0.2
6500	19479.8	0.0	17594.7	0.0	17594.7	0.0	19479.8	0.0	16966.3	0.0
7000	3141.9	0.0	3141.9	0.0	3141.9	0.0	2513.5	0.0	3141.9	0.0
7500	1256.8	0.0	1256.8	0.0	1256.8	0.0	1256.8	0.0	1256.8	0.0
8000	628.4	0.0	628.4	0.0	628.4	0.0	628.4	0.0	628.4	0.0
Total	53308323.6	100.0	54358725.6	100.0	53864042.9	100.0	52475113.4	100.0	54478908.3	100.0
			2011_04		2010_04		2009_04		2008_04	
Contour	Area	%								
0	10999024.2	30.4	7878629.6	23.5	9080069.2	26.9	7997883.2	24.8	8436200.9	26.5
500	6764994.4	18.7	13234929.7	39.4	4685703.7	13.9	7064639.2	21.9	5465795.2	17.2
1000	3436179.6	9.5	3521242.5	10.5	5145792.3	15.3	2824878.9	8.8	3415148.5	10.7
1500	8661662.3	24.0	2653021.0	7.9	7965703.4	23.6	7551817.1	23.4	2296278.4	7.2
2000	1919586.5	5.3	1469056.9	4.4	2054501.5	6.1	2015961.6	6.2	1909271.0	6.0
2500	869231.9	2.4	1361802.1	4.1	886655.9	2.6	1335973.3	4.1	6460291.5	20.3
3000	548500.3	1.5	552940.8	1.6	1021159.8	3.0	536248.4	1.7	1026730.1	3.2
3500	368967.9	1.0	355960.5	1.1	349032.5	1.0	363113.1	1.1	348273.2	1.1
4000	342367.1	0.9	319343.4	1.0	335367.3	1.0	354689.3	1.1	337351.4	1.1
4500	594704.9	1.6	573096.7	1.7	559153.8	1.7	580175.6	1.8	531475.6	1.7
5000	956298.9	2.6	993456.0	3.0	935009.0	2.8	947195.9	2.9	957132.0	3.0
5500	521782.1	1.4	508988.5	1.5	543753.1	1.6	528694.3	1.6	522184.5	1.6
6000	135730.3	0.4	136987.0	0.4	128818.1	0.4	135730.3	0.4	136358.6	0.4
6500	17594.7	0.0	18851.4	0.1	16966.3	0.1	18223.0	0.1	17594.7	0.1
7000	3141.9	0.0	3141.9	0.0	3141.9	0.0	3141.9	0.0	3770.3	0.0
7500	1256.8	0.0	1256.8	0.0	1256.8	0.0	628.4	0.0	1256.8	0.0
8000	628.4	0.0	628.4	0.0	628.4	0.0	628.4	0.0	628.4	0.0
Total	36141652.0	100.0	33583333.0	100.0	33712712.8	100.0	32259621.6	100.0	31865740.9	100.0
			2011_07		2010_07		2009_07		2008_07	
Contour	Area	%								
0	24977.1	5.1	16251.0	3.2	22070.7	3.6	17640.8	3.7	19238.2	3.7
500	9376.2	1.9	5903.8	1.2	4172.7	0.7	4828.9	1.0	6057.8	1.2

1000	3766.8	0.8	0.0	0.0	0.0	0.0	1486.4	0.3	0.0	0.0
1500	2717.8	0.6	1885.1	0.4	1885.1	0.3	3164.3	0.7	2513.5	0.5
2000	4927.9	1.0	3494.8	0.7	3494.8	0.6	2640.4	0.5	2238.0	0.4
2500	3374.0	0.7	3374.0	0.7	6714.0	1.1	1256.8	0.3	628.4	0.1
3000	17821.4	3.7	4172.7	0.8	20510.6	3.4	6686.2	1.4	6686.2	1.3
3500	21783.6	4.5	10230.5	2.0	21139.0	3.5	16740.3	3.5	16111.9	3.1
4000	25537.6	5.2	10230.5	2.0	24683.3	4.1	16111.9	3.4	14855.2	2.8
4500	36174.2	7.4	29109.8	5.8	34737.4	5.7	26568.4	5.5	29533.9	5.7
5000	159247.9	32.7	207542.1	41.2	230191.7	37.9	191164.9	39.8	223048.0	42.7
5500	119869.5	24.6	149102.7	29.6	181150.1	29.8	140140.4	29.2	152697.2	29.3
6000	49246.4	10.1	53054.7	10.5	46500.2	7.6	42377.8	8.8	40100.9	7.7
6500	6686.2	1.4	6283.8	1.2	6912.2	1.1	7314.6	1.5	6283.8	1.2
7000	628.4	0.1	628.4	0.1	1885.1	0.3	1256.8	0.3	628.4	0.1
7500	628.4	0.1	1285.1	0.3	1256.8	0.2	628.4	0.1	628.4	0.1
8000	628.4	0.1	628.4	0.1	628.4	0.1	628.4	0.1	628.4	0.1
Total	487391.7	100.0	503177.3	100.0	607931.9	100.0	480635.6	100.0	521878.2	100.0
		2011_09		2010_10		2009_10		2008_10		2007_10
Contour	Area	%								
0	111976.6	6.8	188062.3	6.4	533296.6	10.9	185548.8	5.9	218392.8	6.7
500	41247.1	2.5	47128.6	1.6	952328.4	19.4	47531.0	1.5	109753.1	3.4
1000	126556.5	7.7	197488.0	6.7	390727.4	8.0	197714.0	6.3	236673.6	7.3
1500	184694.4	11.2	417068.5	14.1	573907.7	11.7	388305.3	12.3	454947.7	14.0
2000	145332.4	8.8	304891.6	10.3	359504.6	7.3	302405.9	9.6	321080.9	9.9
2500	112882.6	6.8	205480.5	6.9	218952.8	4.5	223351.5	7.1	249665.3	7.7
3000	100544.6	6.1	149656.5	5.1	185774.7	3.8	169803.2	5.4	176804.6	5.4
3500	50474.8	3.1	105568.0	3.6	121933.7	2.5	115423.9	3.7	117507.2	3.6
4000	50877.1	3.1	86920.8	2.9	120108.8	2.5	103484.7	3.3	117683.6	3.6
4500	87929.9	5.3	214935.6	7.3	300326.2	6.1	275859.2	8.8	225362.6	6.9
5000	352463.8	21.3	610560.2	20.6	694321.3	14.2	678827.7	21.5	592111.2	18.2
5500	214404.7	13.0	342467.6	11.6	362801.7	7.4	364863.3	11.6	341210.8	10.5
6000	59696.2	3.6	78547.6	2.7	73520.6	1.5	87570.9	2.8	80432.7	2.5
6500	8169.0	0.5	8169.0	0.3	9425.7	0.2	8169.0	0.3	8797.3	0.3
7000	1885.1	0.1	1885.1	0.1	1885.1	0.0	1885.1	0.1	1885.1	0.1
7500	1256.8	0.1	1256.8	0.0	1256.8	0.0	1256.8	0.0	1256.8	0.0
8000	628.4	0.0	628.4	0.0	628.4	0.0	628.4	0.0	628.4	0.0
Total	1651019.9	100.0	2960714.9	100.0	4900700.4	100.0	3152628.5	100.0	3254193.8	100.0

Table 2: Snow cover area in km² on 500m elevation intervals from 0 to 8500m for January, April, July and October months from 2007 to 2011.

13. Khorram S et.al. (1999) Accuracy Assessment of Remote Sensing-Derived Land Cover Change Detection, Monograph, ASPRS, Bethesda, Maryland, 64.
 14. Boori MS, Amaro VE (2011) A remote sensing approach for vulnerability and environmental change in Apodi valley region, Northeast Brazil. World Academy of Science, Engineering and Technology (WASET), International Science Index 50, International journal of Environmental, Earth Science and Engineering 5: 01-11.
 15. Boori MS (2010) Coastal vulnerability, adaptation and risk assessment due to environmental change in Apodi-Mossoro estuary, Northeast Brazil. International Journal of Geomatics and Geosciences 1: 620-638.
 16. Boori MS, Amaro VE, Vital H (2010) Coastal ecological sensitivity and risk assessment: A case study of sea level change in Apodi River (Atlantic Ocean), Northeast Brazil. World Academy of Science, Engineering and Technology (WASET), International Science Index 47, International journal of Environmental, Earth Science and Engineering 4: 44-53.
 17. Nevtipilova V, Pastwa J, Boori MS, Vozenilek V (2014) Testing artificial neural network (ANN) for spatial interpolation. International Journal of Geology and Geosciences 3: 1-9. Doi:10.4172/2329-6755.1000145
 18. Boori MS, Amaro VE (2010) Detecting and understanding drivers of natural and eco-environmental vulnerability due to hydro geophysical parameters, ecosystem and land use change through multispectral satellite data sets in Apodi estuarine, Northeast Brazil. International Journal of Environmental Sciences 1: 543-557.
 19. Boori MS, Amaro VE (2010) Land use change detection for environmental management: using multi-temporal, satellite data in Apodi Valley of northeastern Brazil. Applied GIS International Journal 6: 1-15.
 20. Sudradjat A, Nai-Yu W, Kaushik G, Ralph F (2011) Prototyping a Generic, Unified Land Surface Classification and Screening Methodology for GPM-Era Microwave Land Precipitation Retrieval Algorithms. J Appl Meteor Climatol 50: 1200-1211.